Successful use of retrograde branched extension limb assembling technique in endovascular repair of pararenal abdominal aortic aneurysm

Jiang Xiong, MD, PhD,[a] Zhongzhou Hu, MD, PhD,[a] Hongpeng Zhang, MD, PhD,[a] Huanming Xu, MSc,[b] Duanduan Chen, PhD,[b] *and* Wei Guo, MD,[a] *Beijing, China*

ABSTRACT

Surgeon-modified retrograde branched extension limb assembling technique and bridged endografts were successfully used to exclude an asymptomatic pararenal abdominal aortic aneurysm and to reconstruct the superior mesenteric artery and bilateral renal arteries in a case with high-grade celiac artery stenosis, nondilated aorta above the superior mesenteric artery, and large lumen below the renal arteries. In patient-specific models for hemodynamics analysis, enhanced flow diversion to visceral arteries up to 6-month follow-up confirmed treatment feasibility; however, endograft configurations could be improved to avoid sharp corners at bifurcations, thereby ensuring smooth flow transport and possibly reducing risk for endograft narrowing or the development of thrombosis. (J Vasc Surg Cases and Innovative Techniques 2017;3:90-4.)

Total endovascular repair of thoracoabdominal aortic aneurysms (TAAAs) or pararenal abdominal aortic aneurysms (PRAAAs) with fenestrated or multibranched stent grafts (SGs) precludes aortic clamping and consequent visceral ischemia and yields encouraging outcomes.[1-10] However, it is time-consuming to customize SGs, and the access is limited by insufficient aortic space above the target visceral arteries, whereas additional access, as in reconstruction of visceral arteries via subclavian artery, increases incidence of stroke and upper extremity artery complications.[4-6] Furthermore, passing the customized SG with multiple branches through the nondilated aorta above visceral arteries is technically difficult in PRAAAs. We here describe a case of successful retrograde revascularization of visceral arteries with modified branched extension limb (BEL) assembling technique in total endovascular repair of PRAAA. This patient consented to the publication of this report.

From the Department of Vascular and Endovascular Surgery, Chinese PLA General Hospital[a]; and the School of Life Science, Beijing Institute of Technology.[b]

Jiang Xiong and Zhongzhou Hu are co-first authors.

The hemodynamic part of this work was supported by National Natural Science Foundation of China (81471752) and National Science & Technology Pillar Program (2015BAI04B03).

Author conflict of interest: none.

Additional material for this article may be found online at www.jvsvenous.org.

Correspondence: Wei Guo, MD, Department of Vascular and Endovascular Surgery, Chinese PLA General Hospital, Beijing 100853, China (e-mail: pla301dml@vip.sina.com).

The editors and reviewers of this article have no relevant financial relationships to disclose per the Journal policy that requires reviewers to decline review of any manuscript for which they may have a conflict of interest.

2468-4287

http://dx.doi.org/10.1016/j.jvscit.2017.02.005

CASE REPORT

A 68-year-old man with history of hypertension, chronic obstructive pulmonary disease, coronary artery disease, and diabetes mellitus presented with an asymptomatic PRAAA. Imaging information of this patient is shown in Fig 1. Computed tomography angiography demonstrated a PRAAA with a maximum diameter of 85 mm just below the superior mesenteric artery (SMA; Fig 1, *a*). The images also revealed a high-grade celiac artery stenosis (Fig 1, *c*). With an American Society of Anesthesiologists score of 3, the patient refused open surgery or hybrid repair and provided informed consent for use, with Institutional Review Board approval, of retrograde branched graft assembling technique to reconstruct the SMA and bilateral renal arteries in total endovascular repair of the PRAAA. A PRAAA three-dimensional printing model was prepared to assist anatomic visualization (Fig 1, *g*), which showed a PRAAA diameter of 28.4 mm and 54.9 mm at the SMA and origin of the renal arteries, respectively. The celiac artery was intentionally covered because of high-grade stenosis at its root.

Zenith extension limbs, one 12 × 12 × 122 mm and two 12 × 12 × 88 mm (Cook Medical, Bloomington, Ind), were modified on site under strict sterile conditions and released from a 14F sheath. A 10-mm hole was made using an electrotome, and a 10- × 25-mm Viabahn covered stent (W. L. Gore & Associates, Flagstaff, Ariz) was sewn in the middle of the fourth strut of the Zenith 12- × 12- × 88-mm endograft with end-to-side anastomosis. The coil was sewn around the anastomosis site, and four radiopaque markers cut from a golden pigtail catheter were sewn along the anastomosis site with a 90-degree interval. The inside edge of the branch tip was attached to the endograft's vertical side using polytetrafluoroethylene suture, with a 45-degree angle between the parent endograft and its branch (Fig 1, *h*). Using the same method, two Zenith 12- × 12- × 122-mm extension limbs with an 8 × 25-mm branch were made (Fig 1, *h*), with the anastomosis site between the fourth and fifth struts, and the inside edge

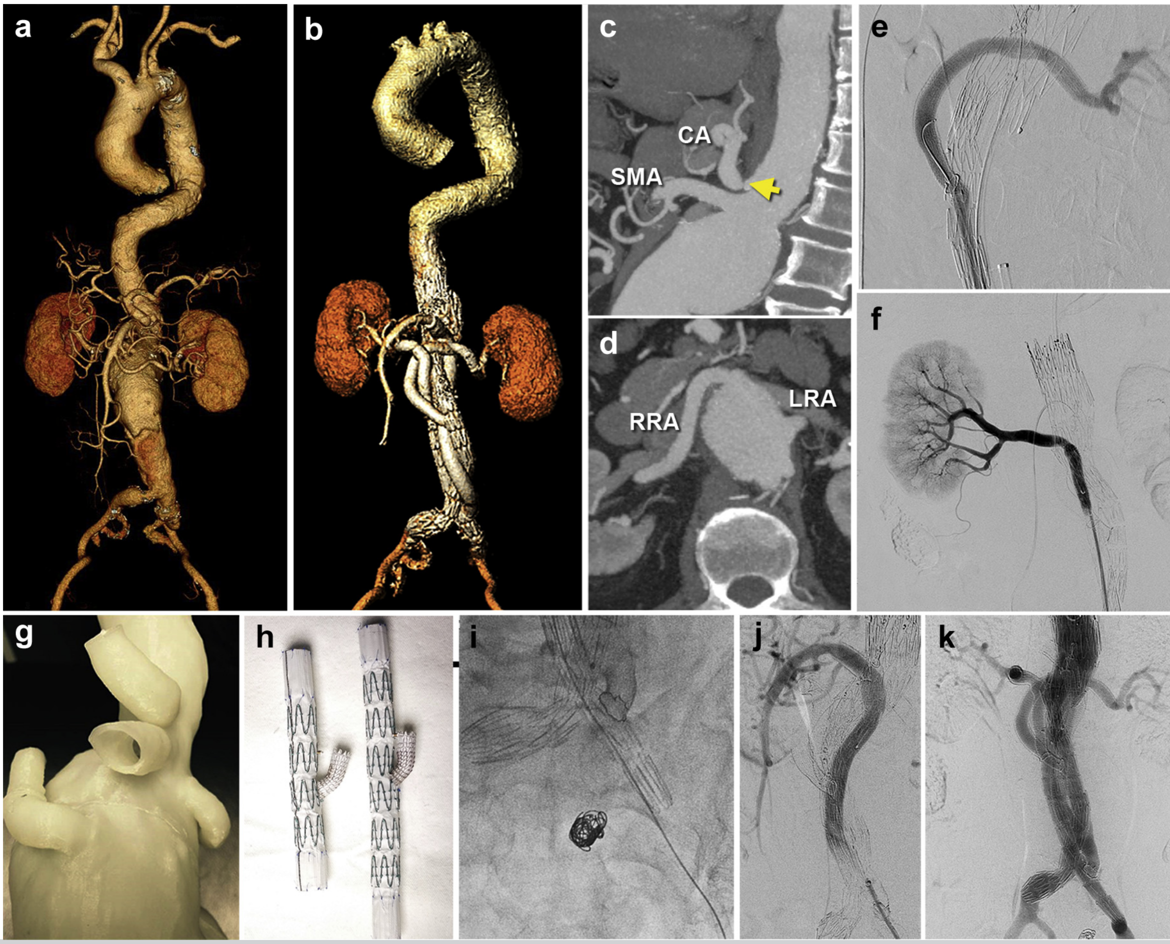

Fig 1. a and **b,** Three-dimensional reconstruction of the aorta based on computed tomography angiography data at initial presentation and after treatment, respectively. **c** and **d,** Roots of celiac artery (*CA*), superior mesenteric artery (*SMA*), left renal artery (*LRA*), and right renal artery (*RRA*); the *arrow* in **(c)** indicates the high-grade stenosis at the origin of the CA. **e** and **f,** Angiography showing the reconstruction of the LRA and RRA, respectively. **g,** Three-dimensional printing model of the aneurysm. **h,** Surgeon-modified branched extension limb (BEL). **i,** Embolization of the left iliac artery. **j,** Reconstruction of the SMA. **k,** Completion aortography revealing patency of all reconstructed visceral branches without endoleak.

of the branch tip was sewn to the endograft's vertical side using polytetrafluoroethylene suture. All modified endografts were reassembled into a 16F introducer sheath. Device modification duration was 160 minutes.

Implantation was performed under general anesthesia in a hybrid operating room (GE Inova 3100-IQ; GE Healthcare, Wauwatosa, Wisc). Bilateral common femoral arteries were surgically exposed, and systemic heparinization was achieved with intravenous bolus injection of 100 IU/kg of unfractionated heparin. Endovascular repair involved the following steps (Fig 2):

1. Through the left femoral approach, a 13 × 100-mm Viabahn covered stent was implanted in the SMA, and the wire was left in the SMA toward the inferior direction to keep the end of the Viabahn stent stable.
2. Through the right femoral approach, a Zenith 36 × 12 × 95-mm bifurcated SG was deployed over a 0.035-inch Lunderquist guidewire (Cook Medical), and the proximal two struts with membrane were deployed over the SMA origin.
3. A modified BEL (12 × 12 × 88 mm) was bridged with a bifurcated SG long limb over a 0.035-inch Lunderquist guidewire.
4. Through the right femoral approach, a left renal artery (LRA) access was established using a 0.035-inch Supra Core guidewire (Abbott Vascular, Santa Clara, Calif) through a modified BEL branch; a 10 × 150-mm Viabahn covered stent was implanted in the LRA; a 10 × 100-mm Viabahn covered stent was bridged between the endograft in the LRA and the modified BEL branch; and the overlap in the modified BEL branch was reinforced with an 8 × 37-mm Express balloon-expandable stent (Boston Scientific, Marlborough, Mass).
5. Through the left femoral approach, a modified BEL (12 × 12 × 88 mm) was deployed in the bifurcated SG short limb with a 3-cm overlap.
6. Through the left femoral approach, using a similar approach as in LRA reconstruction, the right renal artery (RRA) was stented and bridged to the modified BEL branch. Through the right femoral approach, an extension limb was deployed to bridge the modified

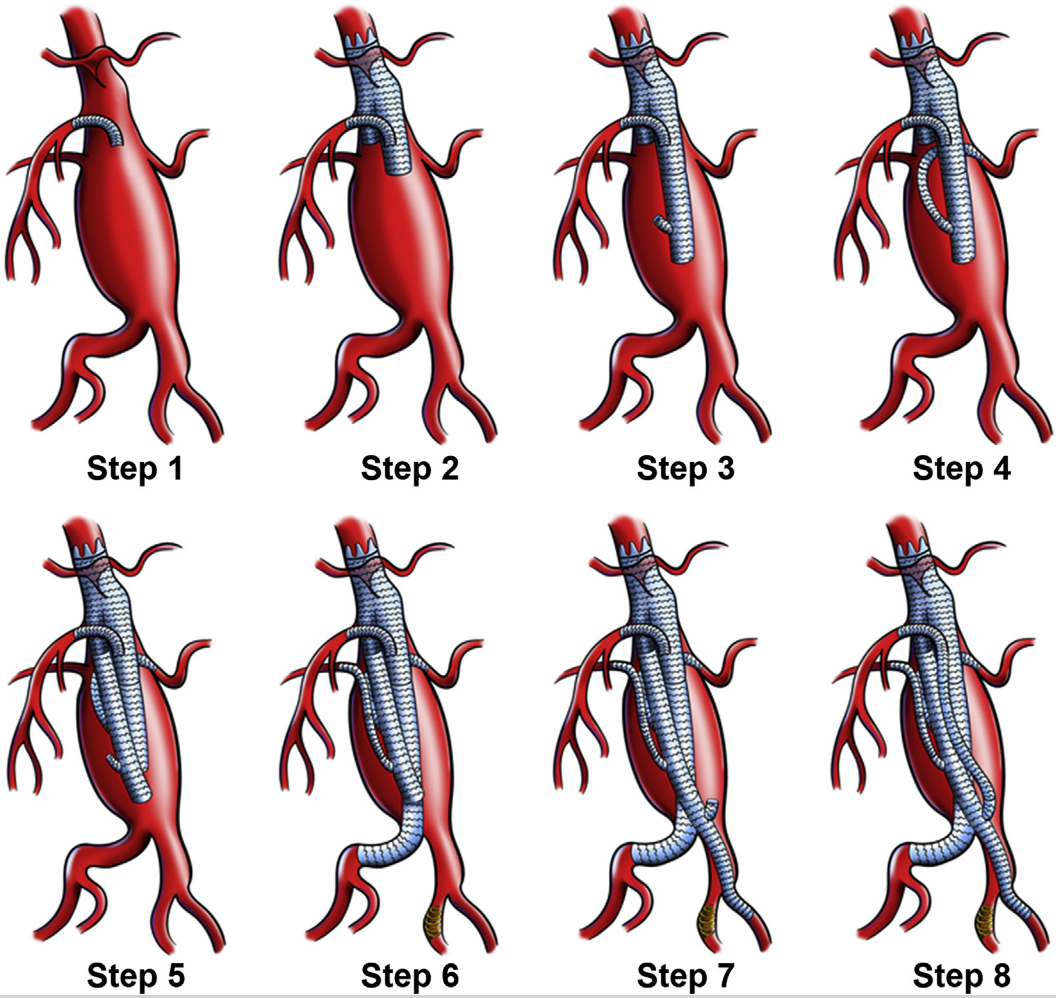

Fig 2. Step-by-step procedure for retrograde branched extension limb (BEL) implantation.

BEL in charge of the LRA to right common iliac artery (RCIA); the left internal iliac artery was then embolized with coils.

7. A modified BEL (12 × 12 × 122 mm) was bridged from the modified BEL in charge of the RRA to left external iliac artery.
8. Through the left femoral approach, using a similar reconstruction technique, the SMA was stented and bridged to the modified BEL branch. All joints and seal zones were inflated with a compliant balloon. Implantation of balloon-expandable stents at each junction was planned intentionally to prevent endograft migration and potential leak between the connected endografts.

Completion angiography revealed exclusion of the aneurysm and patency of BELs without endoleak (Fig 1, *e* and *f*, *i-k*). Procedure and fluoroscopy duration was 300 and 90 minutes, respectively, with 200 mL of total blood loss and 300 mL of total iodinated contrast volume. The patient was discharged on postoperative day 12 without complications. Six-month follow-up computed tomography angiography demonstrated the patency of endografts. There was no type I or type II endoleak in the BEL, endograft migration, or reduced aneurysmal sac (Fig 1, *b*).

To evaluate the effectiveness of endovascular repair, hemodynamic studies were conducted both before treatment and 6 months after treatment (Fig 3 and Supplementary data, online only). Pressure drop distributions at systolic peak (from ascending aorta to common iliac arteries) for the patient vs a normal control (Fig 3, *a* and *b*) and flow patterns at systolic peak (streamlines drawn tangential to instantaneous velocity; Fig 3, *c*) suggested highly vortical flow presence at initial presentation, disrupting visceral flow supply, inducing high-energy exchange, and leading to a low-pressure drop from the distal thoracic aorta to the iliac bifurcation (*arrow*, Fig 3, *a*). After treatment, a relatively organized flow was observed in the endografts (Fig 3, *c*), and pressure at systolic peak in the aorta above the renal arteries gradually dropped from the ascending aorta downstream. Analyses with 100% inflow at the ascending aorta inlet revealed the following flow division (Fig 3, *e*): 8.7% to SMA (6.7% in control); balanced blood supply to bilateral renal arteries (RRA 9.4%, LRA 9.5%; control: RRA 2.7%, LRA 2.9%); and smaller blood transport to left common iliac artery (LCIA;

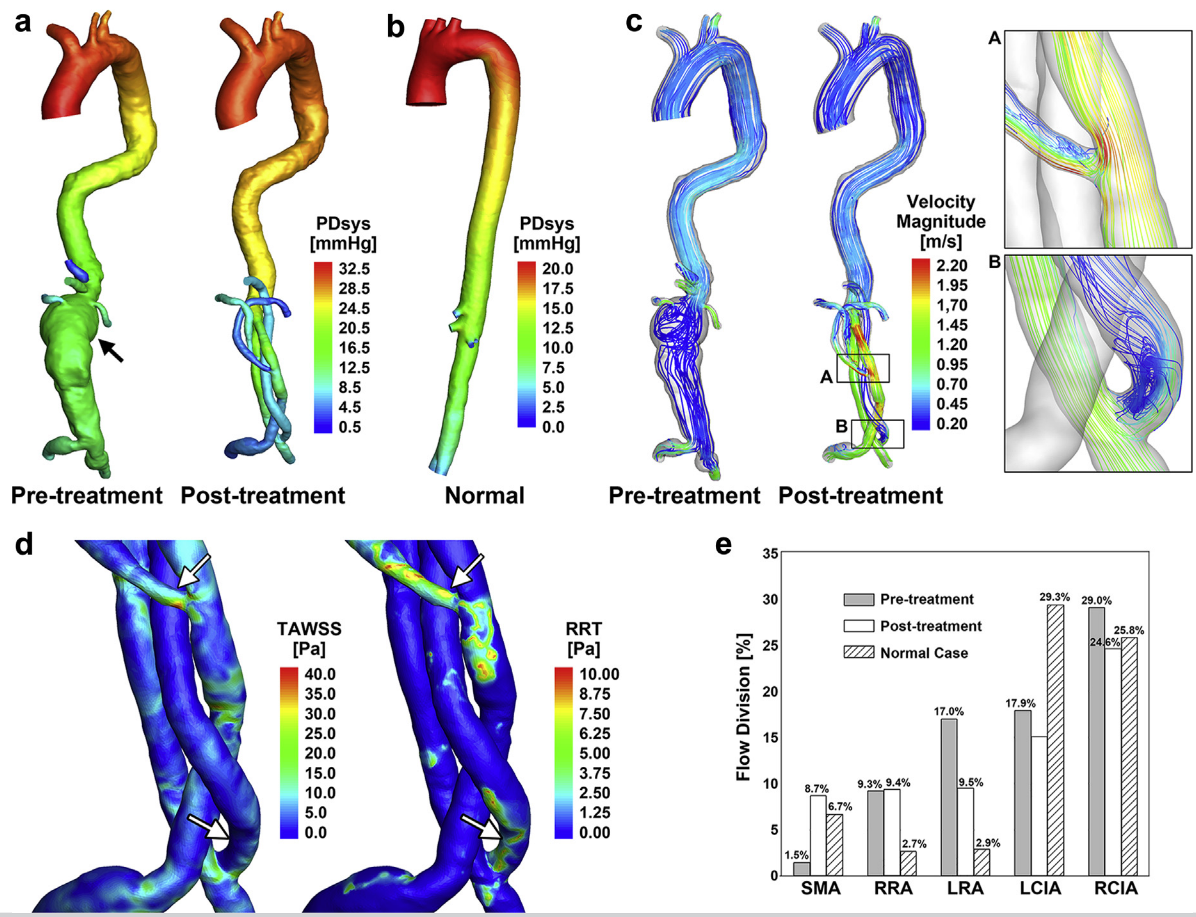

Fig 3. Hemodynamic evaluation of the endovascular repair. **a** and **b,** Pressure drop at systolic peak (*PDsys*) for the patient's case before and after treatment as well as for a normal case. **c,** Flow pattern by drawing the streamlines in the aorta; the magnified images (*A* and *B*) show the vortical flows near the root of the branches. **d,** Distributions of time-averaged wall shear stress (*TAWSS*) and relative residence time (*RRT*) in the abdominal region after treatment; *arrows* indicate the regions with relatively low TAWSS and high RRT. **e,** Flow divisions at the visceral branches and the common iliac arteries. *LCIA,* Left common iliac artery; *LRA,* left renal artery; *RCIA,* right common iliac artery; *RRA,* right renal artery; *SMA,* superior mesenteric artery.

supplying both SMA and RRA) vs RCIA (LCIA 15.1%, RCIA 24.6%; control: LCIA 29.3%, RCIA 25.8%). Vortical flow was present at branched endografts (magnified in Fig 3, *c*), and high relative particle residence time (RRT) corresponded to low time-averaged wall shear stress near the root of BELs (Fig 3, *d, arrows*; Supplementary data, online only).

DISCUSSION

Based on the anatomic features of this patient's case—small space over but large space below intent-construction visceral arteries—retrograde BEL was assembled to reconstruct visceral arteries through femoral access; directional branch was made to the extension limb through which the endografts were bridged to the target vessels. Compared with the upper limb artery antegrade access to visceral arteries, this technique eliminates the requirement of a large space above visceral arteries and reduces the risks of upper limb artery and cerebrovascular complications, and it thus might be suitable for some PRAAAs and type IV TAAAs with insufficient space above the intent-reconstruction visceral arteries. Indeed, more visceral vessel reconstruction would require a wider aneurysmal lumen, and longer aneurysms offer more space for BELs. Thus, patients with wider and longer aneurysmal lumen might be more suitable for the retrograde BEL assembling technique. Moreover, for emergent visceral artery reconstruction, retrograde BEL assembling might allow endovascular repair of TAAAs and PRAAAs with relatively easy-to-manufacture off-the-shelf products and lower endoleak risk than with the chimney or sandwich technique.[11,12]

Based on flow analysis (Fig 3, *e*), blood supply to the SMA was greatly improved, supplying balanced flow to bilateral renal arteries, which would indicate treatment feasibility in terms of visceral blood supply. After treatment, pressure gradually decreased from ascending aorta downstream; however, pressure drop at systolic peak was relatively high in the patient both before and after treatment (Fig 3, *a* and *b*), underscoring the importance of continuous blood pressure control despite pressure drop distribution improvement after endovascular repair. Moreover, low wall shear stress and high RRT are generally believed to be associated with the development of thrombosis in arteries.[13,14] In this case, regional vortices corresponding to low time-averaged wall shear stress and high RRT were found near endograft bifurcations (Fig 3, *c* and *d*), which might possibly predict endograft narrowing or thrombosis, suggesting that attention should be paid at follow-ups to regions near the root of BELs.

CONCLUSIONS

The retrograde BEL assembling technique was successfully used to reconstruct visceral arteries and for total endovascular repair of a patient with PRAAA. Hemodynamic analysis confirmed the improvement of visceral flow supply. Nevertheless, wall shear stress analysis suggested that configurations of the endografts could be further improved to avoid sharp corners at bifurcations, thereby ensuring smoother flow transport and reducing the risk for narrowing in the endograft or the development of thrombosis.

We acknowledge Dr Bo Jiang, Division of Cardiology, University of North Carolina (Chapel Hill, NC), for revising the grammar, syntax, and style of this paper.

REFERENCES

1. Chuter TA, Rapp JH, Hiramoto JS, Schneider DB, Howell B, Reilly LM. Endovascular treatment of thoracoabdominal aortic aneurysms. J Vasc Surg 2008;47:6-16.
2. Kitagawa A, Greenberg RK, Eagleton MJ, Mastracci TM, Roselli EE. Fenestrated and branched endovascular aortic repair for chronic type B aortic dissection with thoracoabdominal aneurysms. J Vasc Surg 2013;58:625-34.
3. Greenberg RK, Lytle B. Endovascular repair of thoracoabdominal aneurysms. Circulation 2008;117:2288-96.
4. Scali ST, Neal D, Sollanek V, Martin T, Sablik J, Huber TS, et al. Outcomes of surgeon-modified fenestrated-branched endograft repair for acute aortic pathology. J Vasc Surg 2015;62:1148-59.e2.
5. Ferreira M, Lanziotti L, Monteiro M. Branched devices for thoracoabdominal aneurysm repair: early experience. J Vasc Surg 2008;48:30S-6S.
6. Ferreira M, Lanziotti L, Cunha R, d'Utra G. Endovascular repair of thoracoabdominal aneurysms: results of the first 48 cases. Ann Cardiothorac Surg 2012;1:304-10.
7. Park JH, Chung JW, Choo IW, Kim SJ, Lee JY, Han MC. Fenestrated stent-grafts for preserving visceral arterial branches in the treatment of abdominal aortic aneurysms: preliminary experience. J Vasc Interv Radiol 1996;7:819-23.
8. Reilly LM, Rapp JH, Grenon SM, Hiramoto JS, Sobel J, Chuter TA. Efficacy and durability of endovascular thoracoabdominal aortic aneurysm repair using the caudally directed cuff technique. J Vasc Surg 2012;56:53-63.
9. Iafrancesco M, Ranasinghe AM, Claridge MW, Mascaro JG, Adam DJ. Current results of endovascular repair of thoracoabdominal aneurysms. Eur J Cardiothorac Surg 2014;46:981-4.
10. Verhoeven EL, Katsargyris A, Bekkema F, Oikonomou K, Zeebregts CJ, Ritter W, et al. Editor's choice—ten-year experience with endovascular repair of thoracoabdominal aortic aneurysms: results from 166 consecutive patients. Eur J Vasc Endovasc Surg 2015;49:524-31.
11. Rouer M, El Batti S, Julia P, de Blic R, Fabiani JN, Alsac JM. Chimney stent graft for endovascular sealing of a pararenal aortic aneurysm. Ann Vasc Surg 2014;28:1936.e15-8.
12. Lobato AC. Sandwich technique for aortoiliac aneurysms extending to the internal iliac artery or isolated common/internal iliac artery aneurysms: a new endovascular approach to preserve pelvic circulation. J Endovasc Ther 2011;18:106-11.
13. Rayz VL, Boussel L, Ge L, Leach JR, Martin AJ, Lawton MT, et al. Flow residence time and regions of intraluminal thrombus deposition in intracranial aneurysms. Ann Biomed Eng 2010;38:3058-69.
14. Gorring N, Kark L, Simmons A, Barber T. Determining possible thrombus sites in an extracorporeal device, using computational fluid dynamics-derived relative residence time. Comput Methods Biomech Biomed Engin 2015;18:628-34.

Submitted Oct 28, 2016; accepted Feb 23, 2017.

Additional material for this article may be found online at www.jvsvenous.org.